Int. J. Heat Mass Transfer. Vol. 24, pp. 285–298
Pergamon Press Ltd. 1981. Printed in Great Britain

0017-9310/81/0201-0285 $02.00/0

DRYOUT AND TWO-PHASE FLOW PRESSURE DROP IN SODIUM HEATED HELICALLY COILED STEAM GENERATOR TUBES AT ELEVATED PRESSURES

H. C. ÜNAL, M. L. G. VAN GASSELT and P. M. VAN 'T VERLAAT
Division of Technology for Society-TNO, P.O. Box 342, 7300 AH Apeldoorn, The Netherlands

(*Received* 19 *March* 1980)

Abstract — The dryout conditions were determined in three sodium-heated circular helically coiled steam generator tubes of 18 mm I.D. The heated straightened lengths of these coils were 40.13, 35.50 and 26.67 m and the coil diameters 0.7 and 1.5 m. The operating conditions of the tests were: pressure: 14.7–20.2 MN/m^2; mass velocity: 112–1829 kg/m^2 s; inlet subcooling: 35.6–156.8 K; dryout steam quality: 0.08–1; dryout heat flux $= 41–731$ kW/m^2. The 203 data obtained for the first and last detected dryouts, the 459 data taken in vertical, long and short electrically heated circular tubes for medium and high pressures and the 215 data taken in a 10 m long, vertical sodium-heated circular tube at high pressures were correlated to predict the dryout heat flux within 20% accuracy for 98% of the time. The RMS-error for all the 877 data was 0.01%.

In the above coils two-phase flow pressure drops were also measured for the following range of operating conditions: pressure: 14.9–20.1 MN/m^2; mass velocity: 296–1829 kg/m^2 s; steam quality at the termination of boiling: 0.15–1. The 70 data obtained and 299 data taken in a 10 m long, vertical, sodium-heated circular tube at high pressures were correlated within 20% accuracy for 98% of the time. The RMS error for all the 369 data was 9.87%.

NOMENCLATURE

A,	cross-sectional area [m^2];
D,	coil diameter [m];
d,	tube inside diameter [m];
f,	friction factor;
G,	mass velocity [kg/m^2 s];
g,	acceleration of gravity [m/s^2];
H,	enthalpy [J/kg];
ΔH,	dimensionless inlet enthalpy [$1 - H_i/H_1$];
L,	length [m];
l,	length of boiling region [m];
n,	number of data;
P,	outlet pressure [N/m^2];
Pr,	reduced outlet pressure (i.e. P divided by critical pressure);
ΔP,	total two-phase flow pressure drop [N/m^2];
ΔP_a,	acceleration pressure drop [N/m^2];
ΔP_f,	frictional pressure drop [N/m^2];
ΔP_g,	gravitational pressure drop [N/m^2];
Q,	developed power [W];
q,	peripheral average heat flux [W/m^2];
r,	radial coordinate [m];
Re,	Reynolds number;
ΔT_{sub},	inlet subcooling [K];
X,	thermodynamic steam quality;
y,	axial coordinate, measured from the inlet of a test tube [m].

Greek symbols

α,	void fraction;
δ,	wall thickness [m];
ρ,	density [kg/m^3];
λ,	latent heat of evaporation [J/kg].

Subscripts

b,	refers to termination of boiling;
d,	refers to dryout location;
e,	refers to equivalent length;
h,	refers to heated length;
i,	refers to inlet condition;
l,	refers to liquid phase at the state of saturation;
m,	refers to measured value;
p,	refers to predicted value;
o,	refers to outlet condition;
v,	refers to vapour phase at the state of saturation.

INTRODUCTION

SODIUM-HEATED helically coiled tube steam generators are used in the LMFBR cooling system. Very little literature exists for the dryout and two-phase flow pressure drop in helically coiled tubes. Below only the work reported in the literature for elevated pressures is mentioned. A literature review deals with the studies made at low pressures [1].

The first systematic analysis of the dryout (or Departure of Nucleate Boiling — DNB) in electrically heated tubes for $P = 17.2$ MN/m^2 is given in [2]. Correlations are reported in [3–5] to determine dryout heat flux and two-phase flow pressure drop in sodium- and electrically-heated helically coiled tubes at medium and high pressures. The correlations given in [3] apply to only two dryout locations and those of [4–5] to one dryout location, probably to the termination of the dryout. As quoted from [2], "the DNB in coiled tubes occurs at different steam qualities for different positions around the circumference of the tube, whereas, for vertical straight tubes DNB occurs around the complete circumference of the tube at one steam quality." In [6], the two-phase flow pressure drop data obtained in three electrically heated helically coiled tubes of $D/d = 46$, 104 and 186 at $P = 17.9\ \mathrm{MN/m^2}$ are compared with the results of six correlations and of these the correlation of [7] gives the best overall agreement.

The present work reports the results of the experiments carried out to determine the dryout conditions and two-phase flow pressure drop in three sodium-heated circular helically coiled tubes of 18 mm I.D. and 26 mm O.D. The heated straightened lengths of these coils were 40.13, 35.50 and 26.67 m and the diameters of the coils 1.5, 0.7 and 0.7 m respectively. Dryout was measured only at the inside (i.e. the side of the tube nearest to the helix axis), top, outside (i.e. the tube surface furthest from the helix axis) and bottom of each tube. The operating conditions of the experiments were: $P = 14.7$–$20.2\ \mathrm{MN/m^2}$; $G = 112$–$1829\ \mathrm{kg/m^2\,s}$; $\Delta T_{sub} = 35.6$–$156.8\ \mathrm{K}$; $X_o = 0.15$–1.61. The 203 data obtained for the first and last detected dryout and the 674 data taken for $P = 4.3$–$20.2\ \mathrm{MN/m^2}$ in vertical, long and short electrically heated circular tubes [8, 9] and in a 10 m long, vertical sodium-heated circular tube [10] were correlated to predict the dryout heat flux within 20% accuracy for 98% of the time. The RMS error for all the 877 data was 9.01%.

In the above coils the two-phase flow pressure drop was also measured for the following range of conditions: $P = 14.9$–$20.1\ \mathrm{MN/m^2}$; $G = 296$–$1829\ \mathrm{kg/m^2\,s}$; $X_b = 0.15$–1.0; $\Delta P = 3.0$–$88\ \mathrm{kN/m^2}$. The 70 data obtained and the 299 data from a 10 m long, vertical sodium-heated circular tube for $P = 14.8$–$19.9\ \mathrm{MN/m^2}$ [10] were correlated to predict the two-phase flow pressure drop within 20% accuracy for 98% of the time. The RMS error for all the 369 data was 9.87%.

EXPERIMENTAL APPARATUS, PROCEDURE AND DATA REDUCTION

Three sodium-heated helically coiled test tubes of 18 mm I.D. and 26 mm O.D. were used. These tubes were manufactured from stainless steel-316 and their total straightened lengths were 44.430, 40.130 and 26.671 m. In the text they are referred to by TT1, TT2 and TT3 respectively. Each test tube was installed in a heat transfer loop, which is described elsewhere [11].

TT1

This 44.43 m long test tube was placed concentrically in another helically coiled tube of 0.049 m I.D. The flow on the sodium side was downward between these coils, and upward in the test tube. A 2.00 m long piece at the inlet and a 2.30 m long piece at the outlet of the test tube were not heated. The coil diameter was 1.5 m and the helix angle was 7.77°.

Both on the sodium- and water/steam-side outlet pressure, mass flow and the temperature along the test tube at $y = 2.000$ (i.e. at the inlet of the heated part of the tube), 8.838, 13.594, 18.350, 23.106, 27.862, 32.618, 34.996, 37.374, 39.752 and 42.130 m (i.e. at the outlet of the heated part of the tube) were measured. The measurement of the pressure drop on the water/steam side was carried out across the successive sections given by the locations $y = 2.000$, 13.594, 23.106, 27.862, 32.618, 37.374 and 42.130 m. In the wall of the last 9.51 m of the heated part of the test tube at the inside, top, outside and bottom, wall temperatures were also measured at 24 axial and 2 radial locations. The coordinates of the latter were $r = 9.75$ and 11.25 mm. Thus the number of measurements for the wall temperatures was 192 for one test run.

TT2

The coil diameter of this test tube was 0.7 m and the helix angle 8.83°. The sodium side surrounding the test tube was constructed of 8 annuli. From the base their respective lengths were 8.829, 6.622, 4.403, 4.403, 4.403, 2.184, 2.184 and 2.184 m. The inner wall of each annulus was formed by the test tube. The I.D. of the outer tube of each annulus was 0.049 m. The annuli were connected by approx. 0.5 m long, U-type, adiabatic circular tubes of 0.049 m I.D. The distance between the two successive annuli was 0.036 m. The flow orientation was upward on the water/steam side and downward on the sodium side. A 4.63 m long piece at the inlet of the test tube was not heated.

Both on the sodium- and water/steam-side outlet pressure, mass flow and the temperature along the test tube at $y = 4.630$ (i.e. at the inlet of the heated part of the tube), 13.459, 20.117, 24.556, 28.995, 33.434, 35.654, 37.873 and 40.130 m and the pressure drop on the water/steam side across the tube sections between two successive values of the above given locations were measured. In the last 10.70 m of the heated part of the test tube measurements of the wall temperatures were carried out at 25 axial locations in a pattern similar to that described for the TT1. Thus in total 200 wall temperatures were measured for one test run.

TT3

This test tube was a short version of the TT2, i.e. the last 26.671 m long part of the TT2 was the TT3. The instrumentation of the latter was identical to that of the TT2.

Type of instruments

Both the sodium- and water/steam-side temperatures were measured with chromel–alumel thermocouples of 1 mm O.D. A similar type of thermocouples of 0.34 mm O.D. was used for the measurements of the wall temperatures. The maximum error in measuring the above-mentioned was 1.2 K.

Both the sodium- and water/steam-side mass flows were measured with turbine flow meters, which had errors less than 1%.

For the measurement of the water/steam-side outlet pressure, a dead-weight balance manometer was used, which had a maximum error of $30\ \mathrm{kN/m^2}$. The pressure drops were measured with pressure transducers, which had an error between about 4 and 10%, with the exception of pressure drops measured for a few test runs carried out at low mass velocities.

Several isothermal and single-phase flow runs were made to calibrate the wall thermocouples. This resulted in the rejection of the temperature measured by some of the wall thermocouples.

All the measurements were collected with an on-line data acquisition system and processed by a Hewlett–Packard-2116B computer. For the tests carried out in TT1, the mass flow and the outlet temperature at the water/steam side and the four wall temperatures measured at the end of the heated part, i.e. at $y = 42.13$ m and $r = 9.75$ mm were simultaneously recorded on a six-line recorder.

Test procedure

In order to determine the dryout conditions, two types of tests were made. In the first type of tests the steam quality at the outlet of a test tube was slowly increased by increasing the sodium-side inlet temperature to about 1 or higher than 1. After reaching the steady-state conditions all the measurements were collected. In the second type of tests, which were only performed in the TT1, the outlet steam quality was increased by small increments by increasing the sodium-side inlet temperature. After each increment and after the steady-state conditions had been reached, all the measurements were collected. By observing the fluctuations in the wall temperatures registered on the multi-channel recorder, the occurrence of the dryout along the circumference of the test tube (i.e. at inside, top, outside and bottom positions) was followed.

Tests were carried out systematically: for a given mass flow and inlet subcooling measurements were made at three pressure levels, mostly at 15, 17.5 and 20 MN/m^2.

Demineralised water with an oxygen content of less than 15 ppb, a conductivity of less than 0.5 μS/cm and a pH between 8.5 and 9 was used during the tests.

Data reduction

All the measurements made were first transformed into a graphical form by plotting the steam quality, peripheral average heat flux and sodium- and water/steam-side temperatures vs the length of a test tube. Smooth curves were drawn through the measured or calculated values. In a graph the wall temperatures were also plotted for the tests carried out in the TT1 and the wall-surface temperatures at the water/steam side for the tests carried out in the TT2 and TT3. For one test run four graphs were then obtained for the inside, top, outside and bottom positions. An example is given in Fig. 1.

The steam quality was calculated with a heat balance. Throughout this study, properties of water, steam and sodium were evaluated from [12] and [13]. For the determination of the peripheral average heat flux the power developed along a test tube was approximated by a 9 or 10th degree polynomial. This power was referenced to the inlet of the test tube.

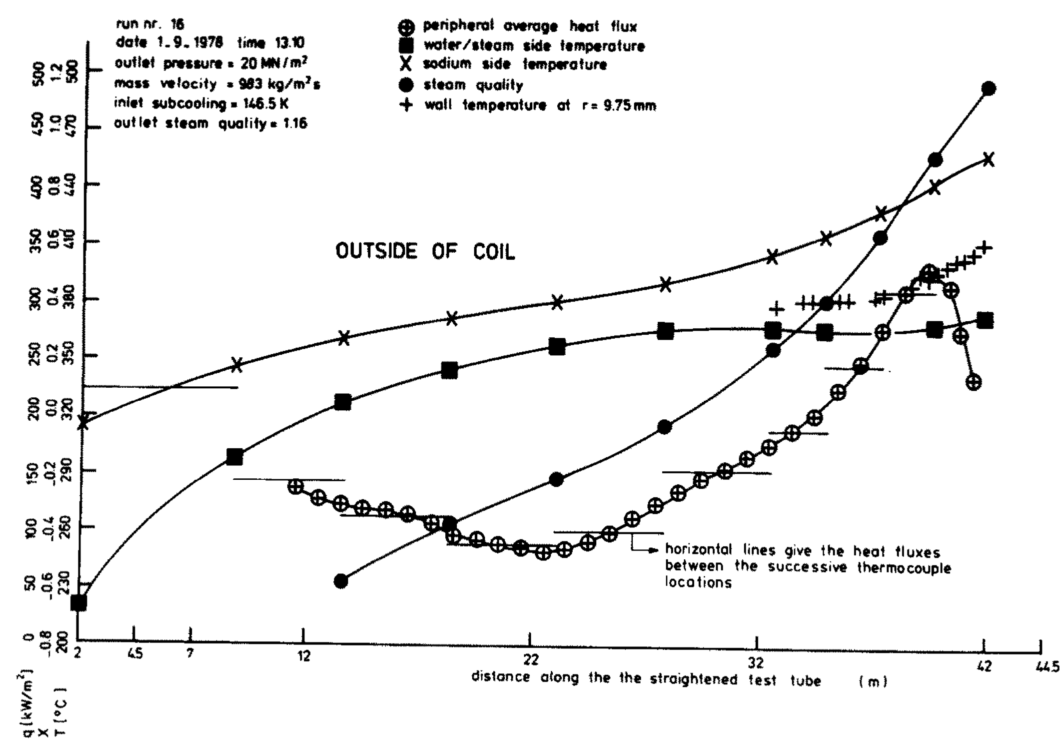

FIG. 1. Plot of measurements.

Thereafter the peripheral average heat flux was determined from this polynomial for each successive meter of the test tube with the formula below

$$q = [Q(y+1) - Q(y)]/\pi d. \quad (1)$$

The value thus determined was then assumed to be valid for the location $(y + 0.5)$ m. The results obtained were checked also with the average heat fluxes calculated for the tube sections between two successive thermocouple locations. Wall surface temperatures at the water/steam side for the tests carried out in the TT2 and TT3 were calculated with the well-known heat conduction formulae.

For the first type of tests, the location of the dryout was determined as follows: Before reaching the dryout, the wall temperatures at $r = 9.75$ mm (or wall surface temperatures at the water/steam side) in the nucleate boiling region were practically constant. After the dryout these temperatures rose. Therefore two wall temperature profiles were drawn in a graph, one before the dryout and the other after the dryout. The axial coordinate of the intersection of these two temperature profiles was assumed to be the location of the dryout. The values of the steam quality and the peripheral average heat flux were then taken from the graph for the aforesaid location.

For the second type of tests, which were carried out only in the TT1, dryout always took place at the end of the test tube. When temperature fluctuations were observed on the multi-channel recorder during a run, the run taken before was considered as the dryout run. The graphs made by a procedure similar to that explained above, for several runs after and before the dryout run, were also consulted to ascertain the determination of the dryout. The peripheral average heat flux at the end of the test tube was predicted with the method explained above.

In both types of tests dryout was only measured at the inside, top, outside and bottom of a test tube.

The methods used to predict the location of dryout appeared to practically eliminate the errors due to mounting the wall thermocouples at the desired coordinates, i.e. $r = 9.75$ mm and 11.25 mm.

For the determination of the two-phase flow pressure drop, the measured values were plotted vs the length of a test tube. A smooth curve was drawn through these values. The two-phase flow pressure drop was then obtained from this curve by assuming that $X = 0$ at the start of boiling and $X = 1$ at the termination of boiling if $X_o \geq 1$.

DISCUSSION OF RESULTS

Dryout always took place in the last quarter length of a test tube. The distance between the locations of the first and last detected dryout varied between 0.2 and 5.1 m. This distance was a small fraction of the length of a test tube, i.e. up to 15%. The above suggests that the location of the first detected dryout nearly coincides with the location where the dryout actually takes place first and the location of the last detected dryout with the location where the dryout in fact terminates. This result is of importance for practical applications.

At mass velocities higher than about 850 kg/m^2 s the dryout was first detected at the inside of a test tube. The last detected dryout was at the outside of the tube. At mass velocities lower than 850 kg/m^2 s, the first and last detected dryouts were at the top and bottom of the tube respectively. As indicated in [2] the location of the dryout appears to depend on, among other things, the centrifugal and gravitational forces.

At high mass velocities wall temperature fluctuations at $r = 9.75$ mm were very small at the first detected dryout location and these fluctuations became larger at the last detected dryout location. Decreasing the mass flow yielded larger temperature fluctuations.

Correlation of the dryout data

Only the data taken for the first and last detected dryouts were considered. The operating conditions for these data are summarized in Table 1.

The present data, the 215 data obtained in a 10 m long, vertical sodium-heated circular tube for $14.8 \leq P$ (MN/m^2) ≤ 20.2 [10] and the 127 data taken in vertical, electrically heated circular tubes of 11 different L_h/d-ratios for $15.7 \leq P$ (MN/m^2) ≤ 19.6 [8] were correlated with the equation below

$$Bo = 0.97\, a_1 a_2 a_3 a_4 a_5/(a_6 a_7), \quad (2)$$

where

$$a_1 = 1 + 3.8\,\Delta H \quad (3)$$

$$a_2 = 0.114 - 0.041 \ln(1 - Pr) \quad (4)$$

$$a_3 = 1 + 4.59(L_e/d)^{-1.2} \quad (5)$$

$$a_4 = 1 + 0.44[\exp(-0.056\,D/d) - \exp(-3\,D/d)]$$

for the first detected dryout (6.1)

$$a_4 = 1 + 0.56[\exp(-0.011\,D/d) - \exp(-3\,D/d)]$$

for the last detected dryout (6.2)

$$a_5 = (2\delta/d)^{0.32} \quad (7)$$

$$a_6 = L_e/d + 28\,Fr^{0.22} \quad (8)$$

$$a_7 = 1. \quad (9)$$

The boiling and Froude numbers in equations (2) and (8) are given below

$$Bo = q_d/(\lambda G) \quad (10)$$

$$Fr = G^2/(9.8\rho_1^2 d). \quad (11)$$

The equivalent length L_e in equations (5) and (8) is per definition

$$L_e \pi d q_d = AG(H_1 - H_i + \lambda X_d). \quad (12)$$

The equivalent length was used in the past by some investigators to take into account the effect on the dryout of the axial non-uniform heat flux distribution and it is based on the following hypothesis: the power

Table 1. Dryout data from TT1, TT2 and TT3

Operating conditions		Test tube TT1	TT2	TT3
First detected dryout	P [MN/m^2]	14.7 – 20.2	14.9 – 20.1	16.8 – 18.5
	G [kg/m^2 s]	112 –1558	116 –1829	387 –1505
	q [kW/m^2]	41 – 712	84 – 612	195 – 367
	X	0.08– 0.64	0.24– 0.79	0.40– 0.43
	ΔT_{sub} [K]	41.2 – 146.9	69.1 – 156.8	35.6 – 79.6
	L_e/d	329 –1293	342 – 989	418 – 620
	n	61	36	2
Last detected dryout	P [MN/m^2]	14.7 – 20.2	14.9 – 20.1	16.8 – 18.5
	G [kg/m^2 s]	112 –1558	116 –1829	387 –1505
	q [kW/m^2]	69 – 691	113 – 731	265 – 445
	X	0.46– 1	0.73– 1.0	0.76– 1.0
	ΔT_{sub} [K]	41.2 – 146.9	69.1 – 156.8	35.6 – 79.6
	L_e/d	357 –1123	395 – 939	500 – 717
	n	65	36	3

developed up to the dryout/burnout point in a non-uniformly heated tube is the same as that of a uniformly heated tube of the same bore and of a hypothetical length found from the condition that in both tubes the local heat fluxes are equal at the dryout/burnout location [14, 15].

The equation (2) is in fact a modification of the correlation given in [16] for vertical electrically heated circular tubes. This correlation is

$$q = 10^4 G[450 + 10^{-3}(H_1 - H_i)] \times [1.02 - (Pr - 0.54)^2]/(40 L_h/d + 156 G^{0.445}) \quad (13)$$

and fits the data obtained at elevated pressures well [9, 16].

For the purpose of this study the above correlation was made non-dimensional and modified by taking the effects on the dryout of coil diameter, wall thickness and axial heat flux distribution: In an electrically heated straight tube the heat flux is in general uniform along the tube, while in a sodium-heated helically coiled or straight tube the heat flux is not uniform along the tube. In a helical coil, dryout appears to be affected by conduction in the tube wall, as observed in [2] and in the present study, and the heat flux varies peripherally. Therefore this effect was taken into account in equation (2) with the parameter given by equation (7). Since bubble formation or the evaporation of a liquid layer on a heated wall is affected by conduction in the wall, the use of this parameter seems also justified for the correlation of data obtained in straight tubes. To the knowledge of the authors the above parameter was not used in any of the numerous empirical dryout correlations presented in the literature. Some of these correlations applicable to medium and high pressures are collected in [9]. Dryout/burnout has been extensively studied in the literature. It is not possible to review all of these studies in this work. The reader is referred to recently published text books.

In order to determine the dryout heat flux and the equivalent length by the use of equations (2) and (12), a simultaneous solution of these equations is not permitted. A kind of an iterative method has to be followed. First the equivalent length has to be solved from equation (12) for a given axial position in a tube. Thereafter this equivalent length has to be inserted into equation (2) to determine the dryout heat flux. This procedure has to be repeated till the calculated dryout heat flux equals the heat flux at the axial location considered.

In short electrically heated straight tubes dryout takes place at the end of the tube [8]. For these tubes $L_e = L_h$, and therefore equation (2) alone is sufficient to determine the dryout heat flux. However, for a vertical sodium heated tube [10] or a vertical electrically heated long tube [9] the dryout does not take place at the end of the tube but somewhere before the end. Therefore for these types of tubes equations (2) and (12) have to be used together for the determination of the dryout heat flux.

With three exceptions, equation (2) predicts the dryout heat flux within 20% accuracy for the present data, the data of [10] and the data of [8] taken for 15.7 $< P$ (MN/m^2) < 19.6. The RMS-error for all the 545 data considered is 8.56%. The ranges of the operating conditions and geometries for the data of [8, 10] are summarized in Table 2. The methods used to obtain the data of [10] are given in [11].

For the derivation of equation (2) the 137 data of [8] obtained in short, vertical electrically heated circular tubes of 21 different L_h/d-ratios for $9.8 \leq P$ (MN/m^2) ≤ 13.7 and 218 data of [9] taken in a long, vertical electrically heated circular tube for $4.3 \leq P$ (MN/m^2) ≤ 16 were not used. With the exception of those taken for low boiling numbers (i.e. 23 data), the aforesaid data of [8] fitted the correlation within the experimental accuracy of the data, i.e. 25% for 95% of the time. In order to restrict the application of the correlation to the above-mentioned 114 data taken for high boiling numbers, the following criteria were established:

$$Pr \geq 0.437 \quad (14.1)$$

Table 2. Dryout data from several investigators

P [MN/m²]	G [kg/m² s]	q [kW/m²]	X	ΔT_{sub} [K]	L^* [m]	d^* [mm]	$\frac{d}{2\delta}$	$\frac{L_e}{d}$	n	Ref.
14.8–20.2	399–3491	131–919	0.25–0.69	18.6–121	10	7.86	1.90	257–759	215	[10]
15.7–19.6	594–5444	613–3582	0–0.334†	7.2–163.3	0.52–1.65	10	5–6.67	52–165	127	[8]
9.8–13.7	492–5542	698–4931	0–0.431†	8–273	0.25–2.1	8–10	4–6.67	25–250	114	[8]
4.3–9.5	1151–2529	184–480	0.433–0.772	29.2–90.2	22	11.8	2.27	1320–1771	99	[9–19]
9.7–16.0	1111–2495	155–418	0.296–0.512	67–135.5	22	11.8	2.27	1500–1827	119	[9–19]

* All the test tubes used were vertical circular tubes.
† True steam quality.

$$Bo(L_e/d)^{0.25}[1 + 0.3(10^{-3}L_e/d)^{4.28}] \geq 3.46 \cdot 10^{-3}(1 - Pr)^{1.11} \quad (14.2)$$

Thus equation (2) is only valid for the conditions given by equations (14.1) and (14.2). The ranges of operating conditions and geometries of the 114 data of [8] taken for $9.8 \leq P$ (MN/m²) ≤ 13.7 are given in Table 2. These data, the present data and data of [8] taken for $15.7 \leq P$ (MN/m²) ≤ 19.6 and the data of [10] satisfy the conditions expressed by equations (14.1) and (14.2).

The 218 data of [9] fitted the correlation within 30 % accuracy, with 6 exceptions. However, all the errors for the data obtained for $P \geq 9.66$ MN/m² were positive, and almost all the errors for the data obtained for $P < 9.66$ MN/m² were negative. In order to correlate these data properly, equation (2) was slightly modified. For this purpose the term a_7 given by equation (9) was transformed into the following forms:

$$a_7 = 1 + 0.049(1 - Pr)^{1.27}(10^{-3}L_e/d)^{4.28} \quad (15.1)$$

$$\text{for} \quad Pr \geq 0.437 \quad (16.1)$$

$$a_7 = [1 + 0.049(1 - Pr)^{1.27}(10^{-3}L_e/d)^{4.28}]/[1.82 - 1.24\,Pr] \quad (15.2)$$

$$\text{for} \quad Pr < 0.437. \quad (16.2)$$

The value of a_7 is practically equal to unity (i.e. within about 0 and 0.7 % accuracy) for the data presented and the data of [8, 10]. This means that the equations (15.1) and (15.2) take into account only the effect on the dryout heat flux of high L_e/d-ratios. This effect is expressed separately for two pressure regions, since in the past several investigators correlated the dryout data obtained at medium and high pressures for two pressure regions as specified roughly by equations (16.1) and (16.2) [16–18]. At $Pr \cong 0.414$, the ratio of the enthalpy of water at the state of saturation to the latent heat of evaporation is unity. This ratio is greater than unity for $Pr > 0.414$ and smaller than unity for $Pr < 0.414$. This is probably why the effect on the dryout heat flux of pressure differs at the vicinity of a particular pressure.

In equation (2) $D = 0$ for vertical tubes and $D = \infty$ for horizontal tubes.

After the above modification the 218 data of [9] fitted the correlation well, i.e. within 19 % accuracy for 99 % of the time with a RMS-error of 8 %. These data satisfy the conditions given by equations (14.1) and (14.2). The ranges of operating conditions and geometries for these data are given in Table 2.

The errors in predicting the dryout heat flux in accordance with the final form of equation (2) are shown vs reduced pressure in Figs. 2(a)–(g) for the data presented and data of [8–10]. The correlation fits the data well, i.e. within 20 % accuracy for 98 % of the time. The RMS-error for all the 877 data was 9.01 %.

This accuracy is considered satisfactory. In order to ascertain this, the 215 data of [10] obtained in a vertical, sodium-heated circular tube were compared

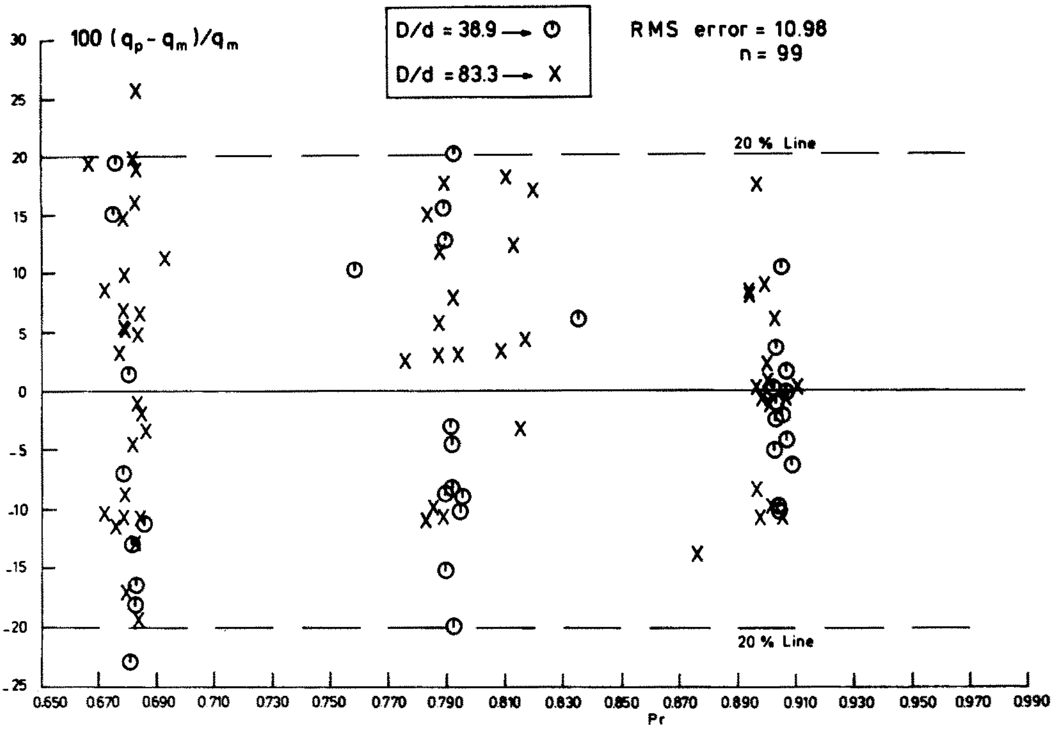

FIG. 2(a). Errors in predicting the heat flux for the first detected dryout.

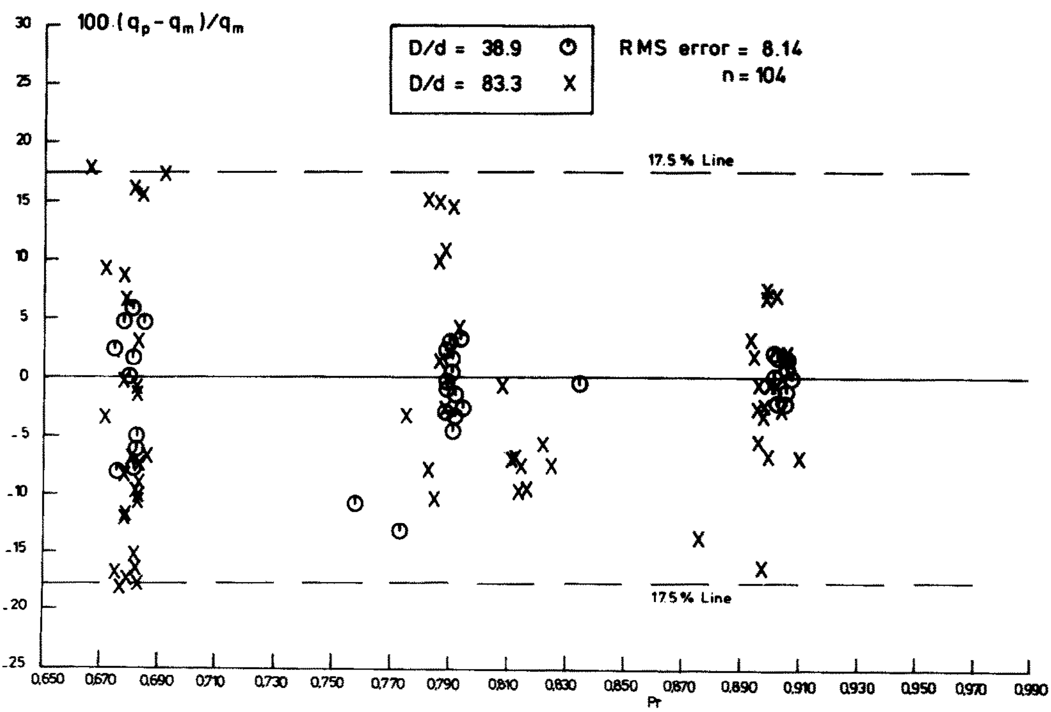

FIG. 2(b). Errors in predicting the heat flux for the last detected dryout.

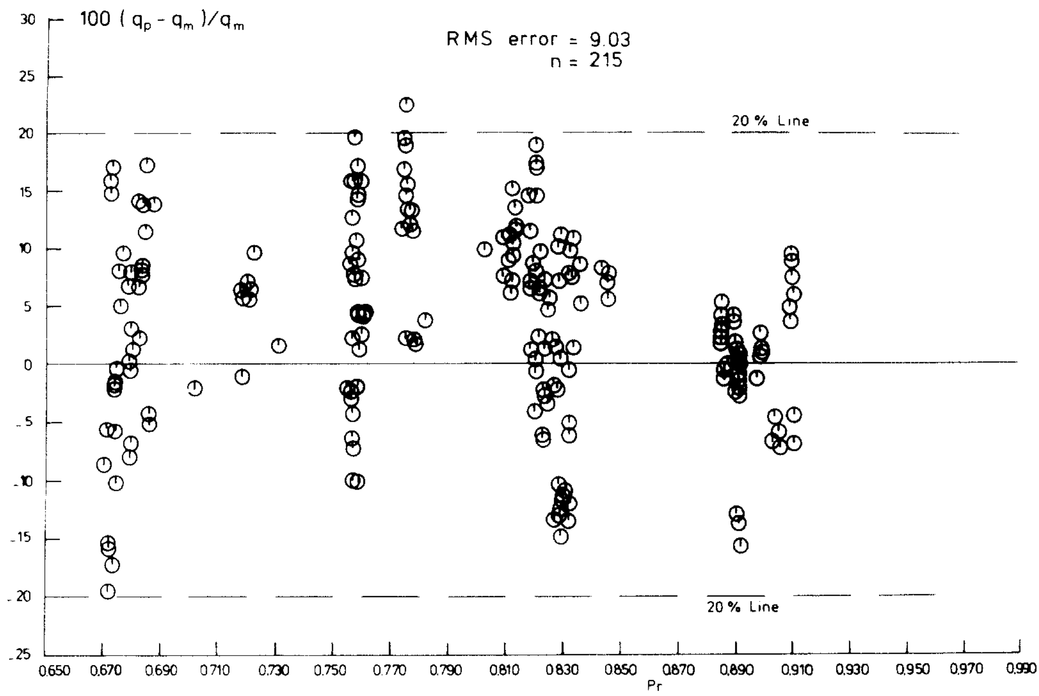

FIG. 2(c). Errors in predicting the dryout heat flux for the data of [10].

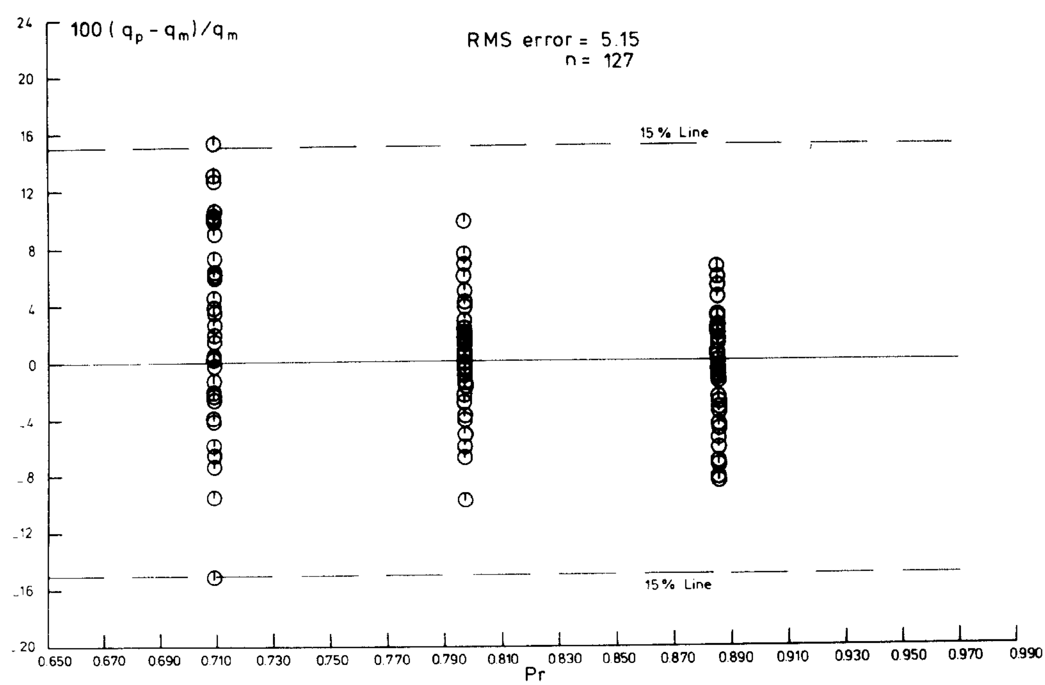

FIG. 2(d). Errors in predicting the dryout heat flux for the data of [8] obtained for $15.7 \leq P\,(MN/m^2) \leq 19.6$

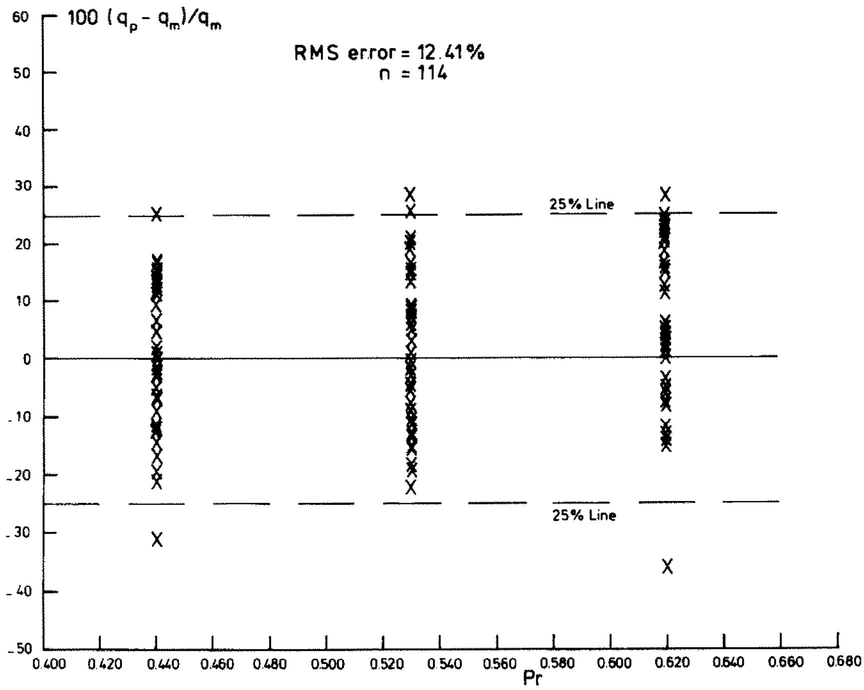

FIG. 2(e). Errors in predicting the dryout heat flux for the data of [8] obtained for $9.8 \leq P\ (\mathrm{MN/m^2}) \leq 13.7$.

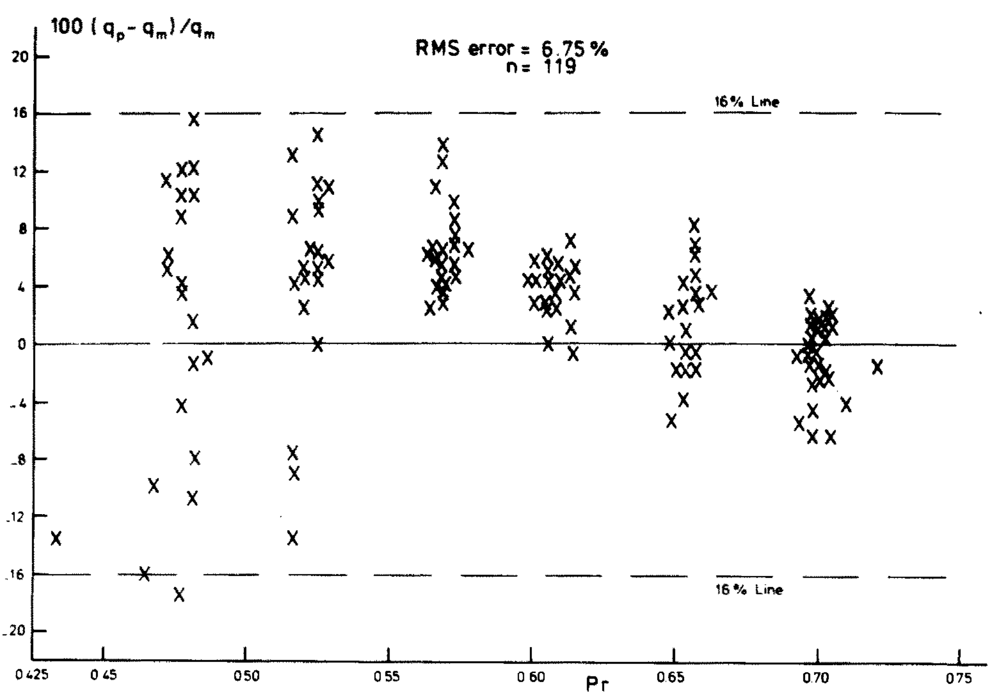

FIG. 2(f). Errors in predicting the dryout heat flux for the data of [9] obtained for $9.7 \leq P\ (\mathrm{MN/m^2}) \leq 16$.

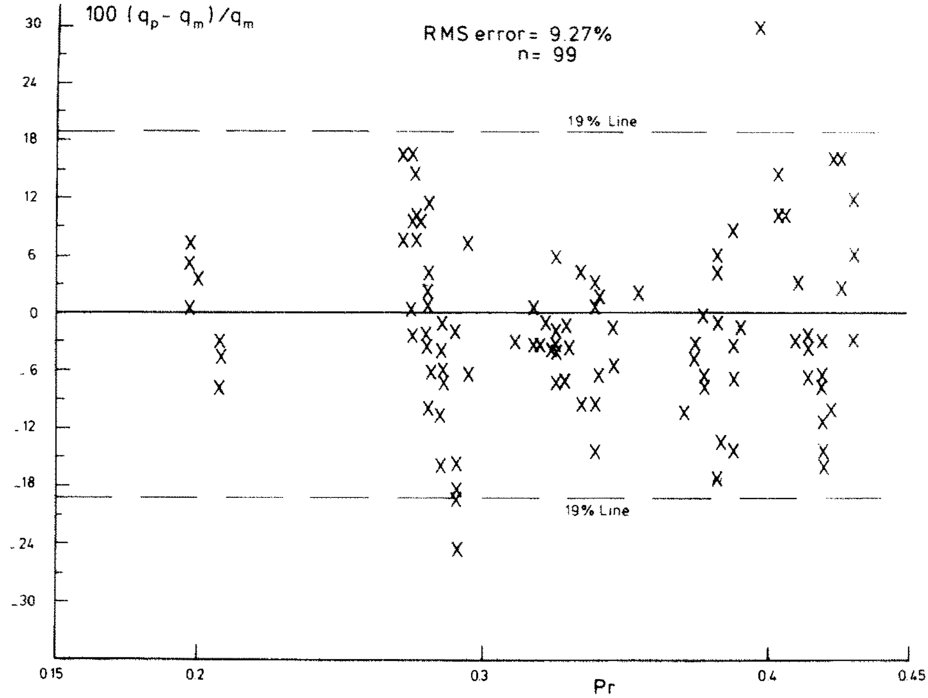

FIG. 2(g). Errors in predicting the dryout heat flux for the data of [9] obtained for $4.3 \leq P$ (MN/m^2) ≤ 9.5.

with the correlations of [16, 8, 20–22], which were derived from the data taken in vertical uniformly heated (i.e. electrically heated) circular tubes at high pressures. The correlation of [16] is given by equation (13). This correlation fitted the data poorly, i.e. the RMS-error in predicting the dryout heat flux was 59.8%. When using L_e/d instead of L_h/d in the correlation, the correlation yielded a RMS-error of 10.7%. However, with 5 exceptions the error was between +8.4 and −29.2%. The correlations of [8, 20–22] also fitted the data poorly, i.e. with a RMS-error of 39.8, 78.9, 103.4 and 111.5%. For the four last-mentioned correlations it was not possible to check the effect of the equivalent length since these correlations do not include the tube length as a correlating parameter. From the above it is quite clear that the correlations based on data obtained in uniformly heated tubes yield very inaccurate results for non-uniformly heated tubes.

The range of geometries and operating conditions of the data used to establish equation (2) are recapitulated below: geometries and heating conditions: sodium-heated helically coiled circular tubes, a vertical sodium-heated circular tube and vertical, short and long electrically heated circular tubes; $L_h = 0.25$–40.13 m; $d/(2\delta) = 1.90$–6.67; $P = 4.3$–20.2 MN/m^2; $G = 112$–5542 kg/m^2 s; $\Delta T_{sub} = 8$–273 K; $X_d = 0$–1; $q_d = 41$–4931 kW/m^2. Equation (2) is not recommended for short tubes for pressures lower than 9.7 MN/m^2 since it has not been verified with the data obtained in these tubes for $P < 9.7$ MN/m^2.

Equations (2) and (6.1) suggest that the effect on the heat flux for the first detected dryout of D/d is quite negligible beyond $D/d = 38.9$. The above ratio clearly affects the heat flux for the last detected dryout, as deduced from equations (2) and (6.1). This seems a logical result since before the last detected dryout most of the tube wall is not wetted by the liquid and the peripheral distribution of the liquid along the wall would, among other things, be a function of D/d. Before reaching the first detected dryout, the whole tube surface is wetted by liquid. It seems therefore that beyond $D/d = 38.9$, the mechanism of dryout in straight tubes is similar to that in helical coils.

Equations (2) and (12) also suggest that the so-called equivalent length hypothesis is of physical importance for the mechanism of dryout.

In order to determine the length between the first and last detected dryout for the sodium-heated helically coiled tubes the well-known heat exchanger formulae will do. The overall heat transfer coefficient is then obtained as the average of the overall heat-transfer coefficients predicted just before the first detected dryout and just after the last detected dryout. With the above procedure the aforesaid length could be predicted within about 1.5% accuracy for the data presented. This accuracy is based on the total tube length.

Correlation of the data for two-phase flow pressure drop

In total 70 data were obtained for two-phase flow pressure drop. The operating conditions for these data are already given in the Introduction.

The data were first compared with the so-called slip

[23] and homogeneous flow models [24]. For this purpose the friction factor of [25] was used:

$$f = 0.079\, Re^{-0.25}\, [Re(d/D)^2]^{0.05}. \quad (17)$$

This correlation applies to the condition, $Re(d/D)^2 > 6$. The slip model fitted the correlation rather well, i.e. between -14.6 and 28.9% accuracy with a RMS-error of 14.5%. The homogeneous flow model fitted the data fairly well, i.e. between -22.8 and 11.4% accuracy with a RMS-error of 7.5%.

The above models were also checked with the 299 data obtained in a 10 m long, vertical sodium-heated circular tube of 7.86 mm I.D. [10]. The operating conditions for these data were: $P = 14.3$–19.9 MN/m^2; $G = 399$–3498 kg/m^2 s; $X_b = 0.06$–1; $\Delta P = 8$–226 kN/m^2. Both of the models fitted these data very poorly. The accuracy of the slip model was between -19 and 115% and that of homogeneous flow model between -23 and 85%. The RMS-errors were 38.7 and 25.9% respectively. Therefore the data presented and the data of [10] were correlated with the equation below

$$\Delta P = \Delta P_a + \Delta P_f + \Delta P_g, \quad (18)$$

where

$$\Delta P_a = \frac{G^2}{\rho_1}\left[\frac{(1 - X_b)^2}{1 - \alpha_b} + \frac{X_b^2}{\alpha_b}\frac{\rho_1}{\rho_v} - 1\right] \quad (19)$$

$$\Delta P_f = 2(1 + b_1 b_2) f_1 1G^2/(d\rho_1) \quad (20)$$

$$\Delta P_g = g\int_0^{\alpha_b} [(1 - \alpha)\rho_1 + \alpha\rho_v]\, dy \quad (21)$$

$$b_1 = 3850\, X_b^{0.2}\, Pr^{-1.515}\, Re_1^{-0.758} \quad (22)$$

$$b_2 = 1 + Re_1^{0.1}(3.67 - 3.04\, Pr)$$
$$\exp(-0.014\, D/d) - \exp(-2D/d)]. \quad (23)$$

For the data presented, the friction factor was evaluated from equation (17) and the void fraction from the correlations given in [26]. Beyond the vapour volumetric rate ratio of 0.57, the flow was assumed to be homogeneous.

For the data of [10], the friction factor was evaluated with the correlations given in [27] and the void fraction with the correlation given in [28]. Beyond the vapour volumetric rate ratio of 0.9, the flow was assumed to be homogeneous.

In order to determine equation (21), it was assumed that the steam quality is a linear function of the axial coordinate and that the pressure is constant in the tube. For the present data the equation (21) had to be determined with a numerical integration method up to vapour volumetric rate ratio of 0.4. For this purpose, the trapezoidal rule was used.

The error in predicting the two-phase flow pressure drop is shown vs reduced pressure in Figs. 3(a) and (b) for the data presented and the data of [10]. The correlation predicts the two-phase flow pressure drops within 20% accuracy for 98% of the time. The RMS-error for all the 369 data is 9.87%.

In equation (18) $D = 0$ for vertical tubes and $D = \infty$ for horizontal tubes.

SUMMARY/CONCLUSIONS

The dryout conditions were determined in three

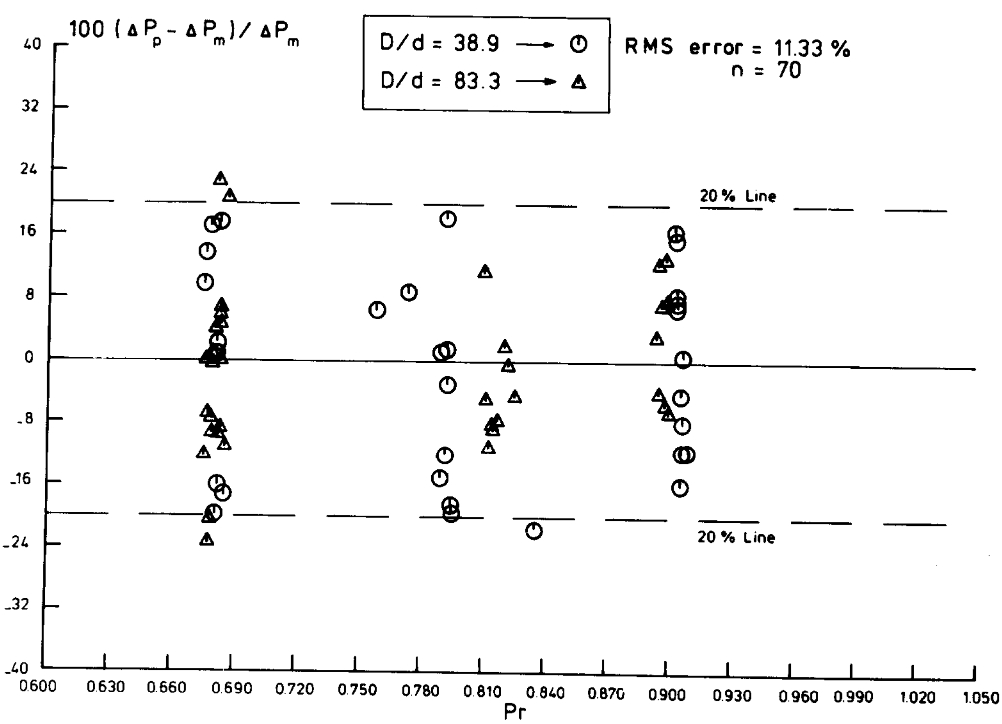

FIG. 3(a). Errors in predicting the two-phase flow pressure drop for the present data.

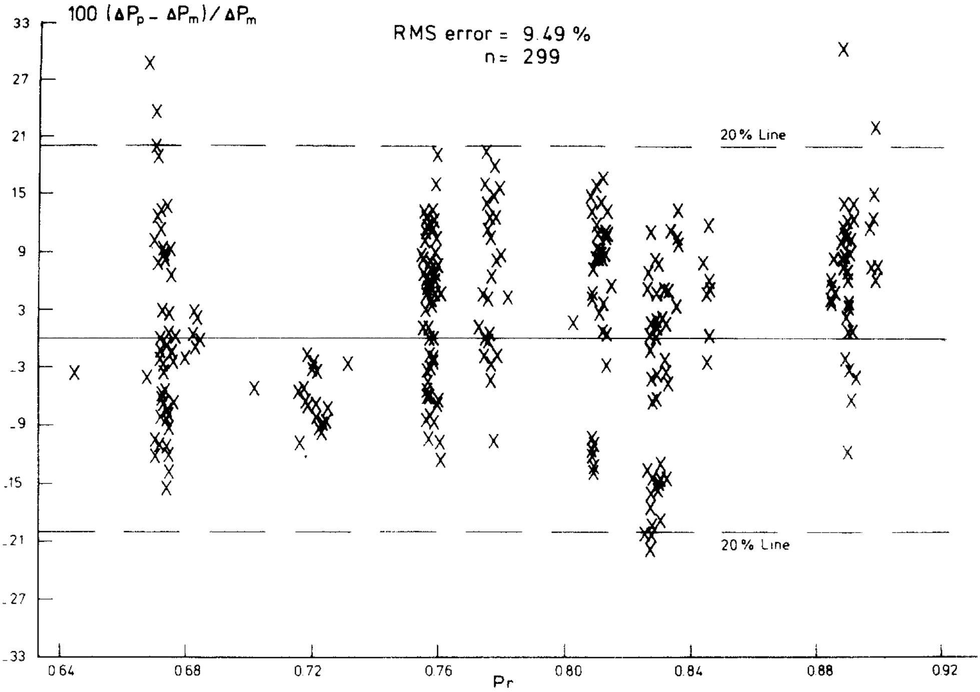

FIG. 3(b). Errors in predicting the two-phase flow pressure drop for the data of [10].

sodium-heated helically coiled circular tubes of 18 mm I.D. The heated straightened lengths of these coils were 40.13, 35.50 and 26.67 m and the coil diameters 1.5, 0.7 and 0.7 m respectively. The tests were carried out for the following range of operating conditions: $P = 14.7\text{–}20.2$ MN/m^2; $G = 112\text{–}1829$ kg/m^2 s; $\Delta T_{sub} = 35.6\text{–}156.8$ K; $X_d = 0.08\text{–}1$; $q_d = 41\text{–}731$ kW/m^2.

The 203 data obtained for the first and last detected dryouts, the 459 data taken in vertical, short and long electrically heated circular tubes and the 215 data taken in a 10 m long, vertical sodium-heated circular tube were correlated to predict the dryout heat flux within 20 % accuracy for 98 % of the time. The RMS-error for all the 877 data is 9.01 %. The ranges of geometries and operating conditions of the data used to establish the correlations are as follows: $L_h = 0.25\text{–}40.13$ m; $d = 7.86\text{–}18$ mm; $d/(2\delta) = 1.90\text{–}6.67$; $D/d = 38.9\text{–}83.3$; $P = 4.3\text{–}20.2$ MN/m^2; $G = 112\text{–}5542$ kg/m^2 s; $\Delta T_{sub} = 8\text{–}273$ K; $X_d = 0\text{–}1$; $q_D = 41\text{–}4931$ kW/m^2. The correlation is not recommended for short tubes for $P < 9.7$ MN/m^2.

For $(D/d) \geq 38.9$, the effect on the heat flux for the first detected dryout of the D/d-ratio seems negligible. The heat flux for the last detected dryout appears to be influenced considerably by the D/d-ratio.

The so-called equivalent length hypothesis would have a physical significance for the mechanism of dryout.

The dryout correlations based on data obtained in uniformly heated (i.e. electrically heated) tubes are not recommended for non-uniformly heated tubes.

In the above coils the two-phase flow pressure drops were also measured. The 70 data obtained and the 299 data taken in a 10 m long, vertical, sodium-heated circular tube of 7.86 mm I.D. were correlated within 20 % accuracy for 98 % of the time. The RMS-error for all the 369 data was 9.87 %. The operating conditions of the data used to establish the correlation is: $P = 14.3\text{–}20.1$ MN/m^2; $G = 296\text{–}3498$ kg/m^2 s; $X_b = 0.06\text{–}1$; $\Delta P = 3.0\text{–}226$ kN/m^2.

Acknowledgements — This study is a government-sponsored work carried out by TNO. The authors wish to express their gratitude to Messrs. K. A. Warschauer, A. R. Braun and G. J. A. M. Meijer for their encouragement. The test tubes were constructed by Messrs. P. H. Engelmann, U. G. Vincent, B. L. Falet and H. Slotboom. The loop was operated by Messrs. A. J. C. Spierings and C. van Huffelen. The maintenance engineer was Mr. R. A. Brand. The on- and off-line computer works were carried out by Messrs. B. J. Stam, R. Vogelzang, G. A. C. Boersen, C. van Huffelen and G. Wentink. The manuscript was typed by Miss M. L. de Ferrante and corrected by Mr. J. D. Duyvensz. The drawings were made by Mr. R. van den Haak.

REFERENCES

1. R. F. Hopwood, Pressure drop, heat transfer and flow phenomena for forced convection boiling in helical coils, a literature survey, AEEW-R-757 (1972).
2. J. R. Carver, C. R. Kakarala and J. S. Slotnik, Heat transfer in coiled tubes with two-phase flow, the Babcock–Wilcox Company Research Center Report, Report No. 4438 (1964).
3. A. E. Ruffell, The application of heat transfer and pressure drop data to the design of helical coil once-through boilers, Paper presented at "Multi-Phase Flow Meeting" in Glasgow (1974).
4. L. Duchatelle, L. de Nucheze and M. G. Robin, Heat

transfer in helical tube sodium heated steam generators, Paper presented at 1975 International Seminar — Future Energy Production — Heat and Mass Transfer Problems, Dubrovnik, 25–30 August (1975).
5. M. Naitoh, A. Nakamura and H. Ogasawara, Dryout in helically coiled tube of sodium heated steam generator, *ASME paper* 74-WA/HT-48 (1975).
6. W. T. Anglease, D. J. B. Chambers and R. C. Jeffrey, Measurement of water/steam pressure drop in helical coils, paper presented at "Multi-Phase Flow Meeting" in Glasgow (1974).
7. C. J. Baroczy, A systemic correlation for two-phase pressure drop, *Chem. Engng Prog. Symp. Ser.* **62**(64), 232–249 (1966).
8. O. L. Peskov, V. I. Subbotin, B. A. Zenkevich and N. D. Sergeyev, The critical heat flux for the flow of steam–water mixtures through pipes, in *Problems of Heat Transfer and Hydraulics of Two-Phase Media*, pp. 48–62 (edited by S. S. Kutateladze). Pergamon Press, Oxford (1969).
9. F. Campolunghi, M. Cumo, G. Ferrari, R. Leo and G. Vaccaro, An experimental study on heat transfer in long, subcritical once-through steam generators, in *Proceedings of International Meeting on Reactor Heat Transfer, Karlsruhe*, pp. 373–403 (9–11 October 1973).
10. P. J. de Munk, A. D. Koppenol and B. J. Stam, Warmteoverdracht- en drukvalmetingen in een natriumverhitte stoomgenerator testsectie in het drukbereik van 150 tot 200 bar, een compilatie van metingen, TNO-Report, Report No. 74-0839 (1974). [Confidential]
11. P. J. de Munk, Two-phase flow experiments in a 10 m long sodium heated steam generator test section, in *Proceedings of International Meeting on Reactor Heat Transfer, Karlsruhe*, pp. 504–518 (9–11 October 1973).
12. The American Society of Mechanical Engineers, *1967 ASME Steam Tables*, New York (1967).
13. M. E. Durham, The thermodynamic and transport properties of liquid sodium, CEGB-Report-RD/B/M2479 (Revised), CFR/THWP/P (72) 28 (Revised) (1964).
14. P. G. Barnett, The prediction of burnout in non-uniformly heated rod clusters from burnout data for uniformly heated round tubes, AEEW-R **362** (1964).
15. D. H. Lee, An experimental investigation of forced convection burnout in high pressure water. Part III — Long tubes with uniform and non-uniform axial heating, AEEW-R **355** (1965).
16. K. M. Becker, Burnout conditions for round tubes at elevated pressures, Paper presented at "International Symposium on Two-Phase Flow Systems", Technion City, Haifa, Israel (1971).
17. K. M. Becker and P. Persson, An analysis of burnout conditions for flow of boiling water in vertical round ducts, *J. Heat Transfer* **86C**, 515–530 (1964).
18. F. Campolunghi, M. Cumo, G. Ferrari and G. Vaccaro, A burnout correlation for once-through L.M.F.B.R. steam generators, CNEN Report-RT/ING (74) 8 (1974).
19. M. Cumo, Personal communication, CNEN, Roma, Italy.
20. A. S. Konkov, Experimental study of the conditions under which heat exchange deteriorates when a steam–water mixture flows in heated tubes, *Teploenergetika* **13**(12), 53–57 (1966).
21. F. E. Tippets, Analysis of the critical heat flux conditions in high pressure boiling water flows, *J. Heat Transfer* **86**, 23–38 (1964).
22. D. H. Lee, Studies of heat transfer and pressure drop relevant to sub-critical once-through evaporators, Paper presented at "IAEA Symposium on Progress in Sodium-Coiled Fast Reactor Engineering", Monaco, 23–27 March (1970).
23. R. C. Martinelli and D. B. Nelson, Prediction of pressure drop during forced-circulation boiling of water, *Trans. Am. Soc. Mech. Engrs* **70**(6), 695–702 (1948).
24. W. L. Owens Jr., Two-phase pressure gradient, *Int. Devel. Heat Transfer, Part* 2, 363–368 (1961).
25. H. Ito, Friction factors for turbulent flow in curved pipes, *J. Bas. Engng* **81**, 123–134 (1959).
26. H. C. Ünal, Determination of void fraction, incipient point of boiling and initial point of net vapor generation in sodium-heated helically coiled steam generator tubes, *J. Heat Transfer* **100**(2), 268–274 (1978).
27. J. G. Knudsen and D. L. Katz, *Fluid Dynamics and Heat Transfer*, pp. 175–176. McGraw-Hill, New York (1958).
28. H. C. Ünal, Determination of the drift velocity and the void fraction for the bubble- and plug flow regimes during the flow boiling of water at elevated pressures, *Int. J. Heat Mass Transfer* **21**, 1049–1056 (1978).

ASSECHEMENT ET PERTE DE PRESSION EN ECOULEMENT DIPHASIQUE DANS UN TUBE HELICOIDAL DE GENERATEUR DE VAPEUR A PRESSION ELEVEE, CHAUFFE PAR DU SODIUM

Résumé—Les conditions d'assèchement sont déterminées pour trois tubes hélicoïdaux de générateur de vapeur chauffés par du sodium et de 18 mm de diamètre intérieur. Les longueurs chauffées de ces serpentins sont 40,13, 35,50 et 26,67 mm et les diamètres des serpentins 0,7 et 1,5 m. Les conditions d'essai sont: pression 14,7–20,2 MN/m^2; débit massique spécifique 112–1829 kg/m^2 s; sous-refroidissement à l'entrée 35,6–156,8 K; qualité de la vapeur à l'assèchement 0,08–1; flux thermique à l'assèchement 41–731 kW/m^2. Les 203 résultats obtenus pour les premiers et derniers assèchements détectés, les 459 données pour les serpentins chauffés électriquement pour des pressions moyennes ou élevées et les 215 données pour un tube vertical de 10 m de longueur chauffé par du sodium sont regroupés pour prévoir le flux thermique d'assèchement à moins de 20% pour 98% des cas. L'écart-type pour tous les 877 cas est de 9,01%.

Dans les serpentins, les chutes de pression de l'écoulement diphasique sont mesurées pour les conditions d'essai suivantes: 14,9–20,1 MN/m^2; débit massique spécifique 296–1829 kg/m^2 s; qualité de la vapeur à la fin de l'ébullition 0,15–1. Les 70 résultats obtenus et les 299 données pour un tube vertical de 10 m, chauffé au sodium sont regroupés à mieux que 20% pour 98% des cas. L'écart-type pour tous les 369 cas est de 9,87%.

DRYOUT UND DRUCKABFALL DER ZWEIPHASENSTRÖMUNG IN NATRIUMBEHEIZTEN SPIRALFÖRMIG GEWICKELTEN DAMPFERZEUGERROHREN BEI HÖHEREN DRÜCKEN

Zusammenfassung — In drei natriumbeheizten runden, spiralförmig gewickelten Dampferzeugerrohren mit dem Innendurchmesser 18 mm wurden die Dryout-Bedingungen untersucht. Die beheizte gestreckte Länge dieser Spiralen war 40,3; 35,50 und 26,67 m, der Spiraldurchmesser 0,7 und 1,5 m. Die Arbeitsbereiche bei den Versuchen waren: Druck: 14,7–20,2 MN/m^2; Massenstromdichte: 112–1829 kg/m^2 s; Unterkühlung am Eintritt: 35,6–156,8 K; Dampfgehalt beim Dryout: 0,08–1; Wärmestromdichte beim Dryout: 41–731 kW/m^2. Die 203 Daten, die für die ersten und letzten festgestellten Dryout-Erscheinungen gemessen wurden, die 459 Daten, die in senkrechten Kreisrohren bei langer und kurzer elektrischer Heizstrecke bei mittleren und hohen Drücken aufgenommen wurden und die 215 Daten, die sich in einem 10 m langen senkrechten natriumbeheizten Kreisrohr bei hohen Drücken ergaben, wurden korreliert, so daß die Dryout-Wärmestromdichte mit 20% Genauigkeit für 98% der Fälle angegeben werden kann. Der quadratische Mittelwert des Fehlers für alle 877 Daten war 9,01%.

In den oberen Spiralen wurde auch der Druckverlust in der Zweiphasenströmung gemessen, und zwar für die folgenden Arbeitsbereiche: Druck: 14,9–20,1 MN/m^2; Massenstromdichte: 296–1829 kg/m^{2}s; Dampfgehalt bei Siedebeginn: 0,15–1. Die 70 Daten, die dabei aufgenommen wurden und die 299 Daten, die sich in einem 10 m langen, senkrechten natriumbeheizten Kreisrohr bei hohen Drücken ergaben, wurden ebenfalls mit 20% Genauigkeit für 98% der Fälle korreliert. Der quadratische Mittelwert des Fehlers für alle 369 Daten war hier 9,87%.

КРИЗИС ТЕПЛООТДАЧИ И ПЕРЕПАД ДАВЛЕНИЯ ПРИ ДВУХФАЗНОМ ТЕЧЕНИИ ЖИДКОСТИ В НАГРЕВАЕМЫХ НАТРИЕМ СПИРАЛЬНЫХ ТРУБКАХ ПАРОГЕНЕРАТОРА ПРИ БОЛЬШИХ ДАВЛЕНИЯХ

Аннотация — Определены условия возникновения кризиса теплоотдачи в трех нагреваемых натрием спиральных трубках парогенератора, имеющих внутренний диаметр, равный 18 мм. Длина спрямленных нагреваемых участков равнялась 40,13 м, 35,50 м и 26,67 м, а диаметры витков составляли 0,7 и 1,5 м. Исследования проводились в диапазоне давлений от 14,7 до 20,2 МН/м^2, массовой скорости: 112–1829 кг/м^{2}сек, недогрева на входе: 35,6–156,8 К, паросодержания при кризисе теплоотдачи: 0,08–1, плотности теплового потока при кризисе теплоотдачи: 41–731 кВт/м^2. Данные (203 значения), полученные для первого и последнего из наблюдавшихся кризисов теплоотдачи, результаты измерений в вертикальных (длинных и коротких) нагреваемых электрическим током кольцевых трубках при умеренном и высоком давлениях (459 значений) и в 10-метровой вертикальной нагреваемой натрием круглой трубе при высоких давлениях (215 значений) коррелировались с целью получения соотношения для расчета теплового потока при кризисе теплоотдачи с точностью до 20% при достоверности 98%. Для всех 877 значений относительная среднеквадратичная погрешность не превышала 9,01%.

В этих же спиральных трубках измерялись перепады давления при двухфазном течении жидкости в диапазоне давлений от 14,9 до 20,1 МН/м^2, массовой скорости: 296–1829 кг/м^{2}сек, паросодержания при прекращении кипения: 0,15–1. Данные (70 значений), полученные на спиральных трубках, и результаты измерений (299 значений) в 10-метровой вертикальной нагреваемой натрием круглой трубе при высоких давлениях коррелировались с точностью до 20%. Для всех 369 значений относительная среднеквадратичная погрешность не превышала 9,87%.